The competition of neutrino energy loss due to the pair, photo-, plasma process at the late stages of stellar evolution

LIU Jing-Jing(刘晶晶)[1)]

(The Department of Physics, Qiongzhou University, Wuzhishan 572200, China)

Abstract Based on the Weinberg-Salam theory, the competition of the Neutrino Energy Loss (NEL) rates due to the pair, photo- and plasma process are canvassed. The ratio factor C_1, C_2 and C_3 which correspond the different contributions of the pair, photo- and plasma neutrino process to those of the total NEL rates are accurately taken into account. The ratio factors are very sensitive to the temperature and density. The ratio factor C_2 always is lower than the ratio factor C_1 and C_3. The pair NEL process is the dominant contribution before the crossed point $O(C_1=C_3=0.45)$ and the plasma NEL process will be the main dominant contribution after the crossed point O. With increasing temperature, the crossed point O will move to the direction of higher density.

Key words NEL, the Weinberg-Salam theory, stellar evolution

PACS 14.60.Lm, 97.60.-s

1 Introduction

The main driving force of stellar evolution is the continuous loss of energy into the surrounding space. Photons are the carriers of the escaping energy during most of a star's lifetime. However it has been recognized that the neutrinos play a key role in stellar evolution since the work of Gamow & Schonberg[1]. In recent years, considerable progress has been made in the studies of the neutrino energy loss (hereafter NEL) and the neutrino reactions at the stages of stellar evolution have been a subject of interest in astrophysics, because neutrinos interact so weakly with matter, they can escape unhindered in circumstances where photons are trapped and lots of messages and energy are taken away from the star by the neutrinos.

Some authors investigated extensively their calculation of the neutrino energy loss rates, such as Fuller, Flower and Newman[2], Liu and Luo[3—6], S. Esposito et al.[7] and Indranath Bhattacharyya[8]. Beaudet, Petrosian, and Salpeter[9], and also Dicus[10], remarked the NEL due to the pair, photo- and plasma neutrino process. The three NEL rates were also investigated by Naoki Itoh et al.[11—14] based on the Weinberg-Salam theory.

In this paper, based on the Weinberg-Salam theory, the pair, photo- and plasma NEL at the late stages of stellar evolution is investigated. We consider the three NEL rates for the wide range of the density and temperature. The present paper is organized as follows. In the next section, the calculation of the pair, photo- and plasma NEL rates is formulated. In Section 3 we will discuss some numerical results on the NEL rates. Some remarks are given in Section 4.

2 The NEL rates

Based on the Weinberg-Salam theory, the pair NEL rates per unit volume per unit time due to the pair neutrino process are written as[10, 15, 16] (We use the natural unit in which $h=c=1$ in this article unless specified explicitly)

$$Q_{\rm pair} = \frac{1}{2}\left[(C_{\rm V}^2+C_{\rm A}^2)+n\left(C_{\rm V}'^2+C_{\rm A}'^2\right)\right]Q^{+}_{\rm pair}+ \frac{1}{2}\left[(C_{\rm V}^2-C_{\rm A}^2)+n\left(C_{\rm V}'^2-C_{\rm A}'^2\right)\right]Q^{-}_{\rm pair}\ . \quad (1)$$

Received 12 December 2007

1) E-mail: liujingjing68@126.com

In this paper we note

$$C_{\rm V}=\frac{1}{2}+2\sin^2\theta_{\rm W};\ C_{\rm A}=\frac{1}{2};\ C'_{\rm V}=1-C_{\rm V};\ C'_{\rm A}=1-C_{\rm A}$$

and $\sin^2\theta_{\rm W}=0.2319\pm0.0005$, the $\theta_{\rm W}$ is the Weinberg angle and the n is the number of the neutrino flavors other than the electron neutrino, whose masses can be neglected compared with kT. According to Ref. [11], the pair neutrino energy loss rates are expressed in units of erg·cm^{-3}·s^{-1} as

$$Q_{\rm pair} = \frac{1}{2}\left[(C_{\rm V}^2+C_{\rm A}^2)+n\left(C_{\rm V}'^2+nC_{\rm A}'^2\right)\right]\times \left[1+\frac{(C_{\rm V}^2-C_{\rm A}^2)+n\left(C_{\rm V}'^2-C_{\rm A}'^2\right)}{(C_{\rm V}^2+C_{\rm A}^2)+n\left(C_{\rm V}'^2+C_{\rm A}'^2\right)}q_{\rm pair}\right]\times g(\lambda)\,{\rm e}^{-2/\lambda}f_{\rm pair}\ , \quad (2)$$

where

$$q_{\rm pair} = (10.7480\lambda^2+0.3967\lambda^{0.5}+1.0050)^{-1.0}\times \left[1+(\rho/\mu_{\rm e})(7.692e+07\lambda^3+ 9.715e+06\lambda^{0.5})^{-1.0}\right]^{-0.3}, \quad (3)$$

$$f_{\rm pair}=\frac{(a_0+a_1\xi+a_2\xi^2)\,{\rm e}^{-c\xi}}{\xi^3+b_1\lambda^{-1}+b_2\lambda^{-2}+b_3\lambda^{-3}}\ , \quad (4)$$

$$g(\lambda)=1-13.04\lambda^2+133.5\lambda^4+1534\lambda^6+918.6\lambda^8\ , \quad (5)$$

$$\xi=\left(\frac{\rho/\mu_{\rm e}}{10^9}\right)\lambda^{-1}\ , \quad (6)$$

$$\lambda=\left(\frac{T}{5.9302\times10^9}\right)=\left(\frac{T_9}{5.9302}\right)\ , \quad (7)$$

where $\rho/\mu_{\rm e}$ is the density in units of g/cm^3 and T is the temperature in units of K, T_9 is the temperature in units of 10^9 K.We use the natural unit in which $h=c=1$ in this article unless specified explicitly. The constant a_0, a_1, a_2, b_1, b_2, b_3 and c will be found in Ref. [12].

The energy-loss rate resulting from the photoneutrino process is expressed as[12]

$$Q_{\rm photo} = \frac{1}{2}\left[(C_{\rm V}^2+C_{\rm A}^2)+n\left(C_{\rm V}'^2+C_{\rm A}'^2\right)\right]\times \left[1-\frac{(C_{\rm V}^2-C_{\rm A}^2)+n\left(C_{\rm V}'^2-C_{\rm A}'^2\right)}{(C_{\rm V}^2+C_{\rm A}^2)+n\left(C_{\rm V}'^2+C_{\rm A}'^2\right)}q_{\rm photo}\right]\times \left(\frac{\rho}{\mu_{\rm e}}\right)\lambda^5 f_{\rm photo}\ , \quad (8)$$

$$q_{\rm photo} = 0.666\,(1+2.045\lambda)^{-2.066}\times \left[1+(\rho/\mu_{\rm e})(1.875\times10^8\lambda+1.653\times10^8\lambda^2+ 8.499\times10^8\lambda^3-1.604\times10^8\lambda^4)^{-1.0}\right]^{-1.0}, \quad (9)$$

$$f_{\rm photo}=\frac{(a_0+a_1\xi+a_2\xi^2)\,{\rm e}^{-c\xi}}{\xi^3+b_1\lambda^{-1}+b_2\lambda^{-2}+b_3\lambda^{-3}}\ , \quad (10)$$

$$b_1=6.290\times10^{-3},\ b_2=7.483\times10^{-3},\ b_3=3.061\times10^{-4}\ , \quad (11)$$

$$c=\begin{cases}0.5654+\log_{10}(T/10^7\ {\rm K}) & \text{for } (10^7\ {\rm K}\leqslant T<10^8\ {\rm K})\\ 1.5654 & \text{for } (10^8\ {\rm K}\leqslant T)\end{cases} \quad (12)$$

$$a_i = \frac{1}{2}c_{i0}+\sum_{j=1}^{5}\left[c_{ij}\cos\left(\frac{5}{3}\pi j\tau\right)+d_{ij}\sin\left(\frac{5}{3}\pi j\tau\right)\right]+ \frac{1}{2}c_{i6}\cos(10\pi j)\quad (i=0,1,2)\ , \quad (13)$$

$$\tau=\begin{cases}\log_{10}(T/10^7) & \text{for } (10^7\ {\rm K}\leqslant T<10^8\ {\rm K})\\ \log_{10}(T/10^8) & \text{for } (10^8\ {\rm K}\leqslant T<10^9\ {\rm K})\\ \log_{10}(T/10^9) & \text{for } (10^9\ {\rm K}\leqslant T)\end{cases}\ , \quad (14)$$

where the numerical values of the coefficients c_{ij} and d_{ij} can be found in Ref. [12].

The NEL rates per unit volume per unit time due to the plasma neutrino process are written as[15—18]

$$Q_{\rm plasma}=\left(C_{\rm V}^2+nC_{\rm V}'^2\right)Q_{\rm V}+\left(C_{\rm A}^2+nC_{\rm A}'^2\right)Q_{\rm A}\ , \quad (15)$$

The vector contribution $Q_{\rm V}$ in Eq. (15) consists of two parts: the contribution of the longitudinal plasma $Q_{\rm L}$ and that of the transverse plasma $Q_{\rm T}$ and has been calculated as[9]

$$Q_{\rm V}=Q_{\rm T}+Q_{\rm L}\ , \quad (16)$$

$$Q_{\rm T} = A_0\left(\frac{h\omega_0}{mc^2}\right)^6\int_0^\infty\frac{|k|^2}{{\rm e}^{h\omega/kT}-1}{\rm d}|k|= A_0\gamma^6\lambda^9\int_\gamma^\infty\frac{x(x^2-\gamma^2)^{1/2}}{{\rm e}^x-1}{\rm d}x, \quad (17)$$

$$Q_{\rm L} = A_0\left(\frac{h}{mc^2}\right)^9\frac{1}{2}\left(\frac{5}{3}\right)^{7/2}\left(\frac{1}{\omega_1}\right)\times \int_{\omega_0}^{a\omega_0}\frac{\omega^{10}(\omega^2-a^2\omega_0^2)^2(\omega^2-\omega_0^2)^{1/2}}{{\rm e}^{h\omega/kT}-1}{\rm d}\omega= A_0\gamma^6\lambda^9\left(\frac{\omega_0}{\omega_1}\right)\frac{1}{2}\left(\frac{5}{3}\right)^{7/2}\times \int_1^a\frac{y^{10}(y^2-a^2)^2(y^2-1)^{1/2}}{{\rm e}^{\gamma y}-1}{\rm d}y\ , \quad (18)$$

where

$$A_0 = \frac{g^2}{48\pi^4\alpha}mc^2\left(\frac{mc^2}{h}\right)\left(\frac{mc}{h}\right)^3= 3.001\times10^{21}{\rm erg/cm^3/s},$$

$$g=\frac{Gm^2c}{h^3},\quad \gamma=\frac{h\omega_0}{kT},\quad \lambda=\frac{kT}{mc^2},$$

$$a=\left[1+\frac{3}{5}\left(\frac{\omega_1}{\omega_0}\right)^2\right]^{1/2},$$

$$\left(\frac{h\omega_0}{mc^2}\right)^2=\frac{4\alpha}{3\pi}\left[2G^+_{-1/2}+2G^-_{-1/2}+G^+_{-3/2}+G^-_{-3/2}\right],$$

$$\left(\frac{h\omega_1}{mc^2}\right)^2=\frac{4\alpha}{3\pi}[2G^+_{-1/2}+2G^-_{-1/2}+G^+_{-3/2}+ G^-_{-3/2}-3G^+_{-5/2}-3G^-_{-5/2}],$$

$$G^{\pm}_n(\lambda,\nu)=\lambda^{3+2n}\int_{\lambda-1}^{\infty}\frac{x^{2n+1}(x^2-\lambda^{-2})^{1/2}}{1+\mathrm{e}^{x\pm\nu}}\mathrm{d}x,$$

$$\nu=\frac{\mu}{kT},\quad G=1.02679\pm0.00002\times10^{-5}h^3/(M^2c).$$

Where α is the fine-structure constant, G is the Fermi coupling constant[18] and M is the mass of a proton, ω_0 and ω_1 are the longitudinal and transverse plasma frequencies in unit of the electron mass m_e.

The axial-vector contribution Q_A is given by[17]

$$Q_\mathrm{A}=1.11\times10^{-9}\left(\frac{\rho}{\mu_\mathrm{e}}\right)^3\xi^{-3}\mathrm{e}^{-0.555\xi}\times \left[\alpha_0+(1.00+\alpha_1\xi^{-1}+\alpha_2\xi^{-5})^{-1}\right],\quad(19)$$

where

$$\alpha_0=3.40\times10^{-3}/(1.00+12.5\lambda^{-2}),$$

$$\alpha_1=7.76+0.055\lambda^{-1},\quad \alpha_2=0.50\lambda^{-0.50}+0.014\lambda^{-4}.$$

We note that the present theory is not valid when the condition $h\omega_0\geqslant 2mc^2$ and the electron nondegeneracy condition are both satisfied. In that case, the decay of a plasmon into an electron-positron pair can not be neglected.

In order to compared with the contribution of the pair, photo- and the plasma neutrino energy process, the factors are defined , all of which is the ratio of the neutrino energy loss comes from the pair, photo- and the plasma neutrino process respectively to that of the total neutrino energy loss rates. Therefore we have

$$Q_\mathrm{total}=Q_\mathrm{pair}+Q_\mathrm{photo}+Q_\mathrm{plasma},\quad(20)$$

$$C_1=Q_\mathrm{pair}/Q_\mathrm{total},\quad(21)$$

$$C_2=Q_\mathrm{photo}/Q_\mathrm{total},\quad(22)$$

$$C_3=Q_\mathrm{plasma}/Q_\mathrm{total},\quad(23)$$

3 Some numerical results on the competition of the NEL rates

Figure 1 shows the pair, photo- and plasma NEL rates as a function of ρ/μ_e for the neutrino flavors $n=2$ at the temperature $T_9=7,8,9,10,11(\times10^9\ \mathrm{K})$ respectively. The density has only a mirror effect on the pair NEL rates when $10^6\ \mathrm{g/cm^3}<\rho/\mu_\mathrm{e}\leqslant 10^8\ \mathrm{g/cm^3}$. It also shows that the photo-NEL rates increase slightly when $10^6\ \mathrm{g/cm^3}<\rho/\mu_\mathrm{e}<10^9\ \mathrm{g/cm^3}$, then decrease greatly. On the other hand, one can see that the plasma NEL rate increases greatly when $10^6\ \mathrm{g/cm^3}<\rho/\mu_\mathrm{e}<10^{13}\ \mathrm{g/cm^3}$, but decreases largely after it gets to the peak value.

The pair NEL rate is strongly dependent of the number density of positrons and electrons. So it is constant at low density and decreases when the electrons become degenerate at high density. The photo-NEL rate is constant at very low density due to $\mathrm{e}^{\pm}$ pair and decreases at very high densities. The plasma NEL rate is a strongly peaked function of ρ/μ_e and dominates the other two processes near its own peak which occurs when $\gamma=h\omega_0/kT$ is somewhat larger than unity.

The numerical results of the total NEL rates will be seen in Fig. 1. One can see that the density has only a mirror effect on the total NEL rates when $10^6\ \mathrm{g/cm^3}<\rho/\mu_\mathrm{e}\leqslant 10^8\ \mathrm{g/cm^3}$. It is due to the fact that the pair NEL process is the dominant contribution to the total NEL and the increased magnitude of the photo-, plasma NEL rates is very slight. However the affection on the total NEL rates is large when $\rho/\mu_\mathrm{e}>10^8\ \mathrm{g/cm^3}$. For example the total NEL rates decrease two orders of magnitude due to the large decrease of the pair, photo- NEL rates and the minor increased magnitude of the plasma NEL rates when $10^8\ \mathrm{g/cm^3}\leqslant\rho/\mu_\mathrm{e}\leqslant 3\times10^9\ \mathrm{g/cm^3}$ and $T_9=7\times10^9$ K. On the other hand, the total NEL rates increase about four orders of magnitude when $3\times10^9\ \mathrm{g/cm^3}\leqslant\rho/\mu_\mathrm{e}\leqslant 4\times10^{12}\ \mathrm{g/cm^3}$ and $T_9=7\times10^9$ K. Because the increased magnitude of the plasma NEL rates is larger than the decrease of the pair, photo- NEL rates under this condition.

Figure 2 shows the ratio factor C as a function of density for types of neutrino flavors $n=2$ at different temperatures. One can see from the four figures that the ratio factor C is very sensitive to the temperature. We also can see from the four figures that the ratio factor C_2 always is lower than the ratio factor C_1 and C_3. We find from Fig. 2 that the pair NEL processes is the dominant contribution compared with the others neutrino energy loss processes which correspond to the density region of $\rho/\mu_\mathrm{e}<10^9\ \mathrm{g/cm^3}$, $\rho/\mu_\mathrm{e}<2.8\times10^9\ \mathrm{g/cm^3}$, $\rho/\mu_\mathrm{e}<5\times10^9\ \mathrm{g/cm^3}$ and $\rho/\mu_\mathrm{e}<10^{10}\ \mathrm{g/cm^3}$. One can see from Fig. 2 that the pair NEL process is dominant contribution before the crossed point O which can tell us the relation of $C_1=C_3=0.45$. With increasing of the temperature, the crossed point O will move to the higher density direction.

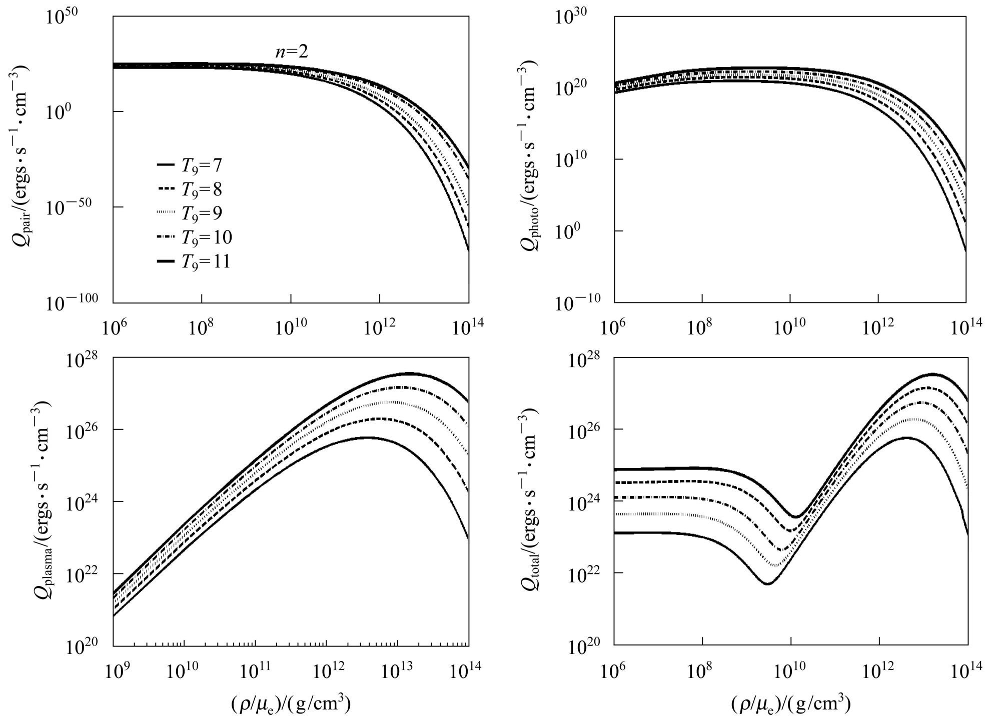

Fig. 1. NEL rates due to the pair, the photo-, the plasma process and the total NEL rates as a function of the density at the different temperatures T_9=7, 8, 9, 10, 11.

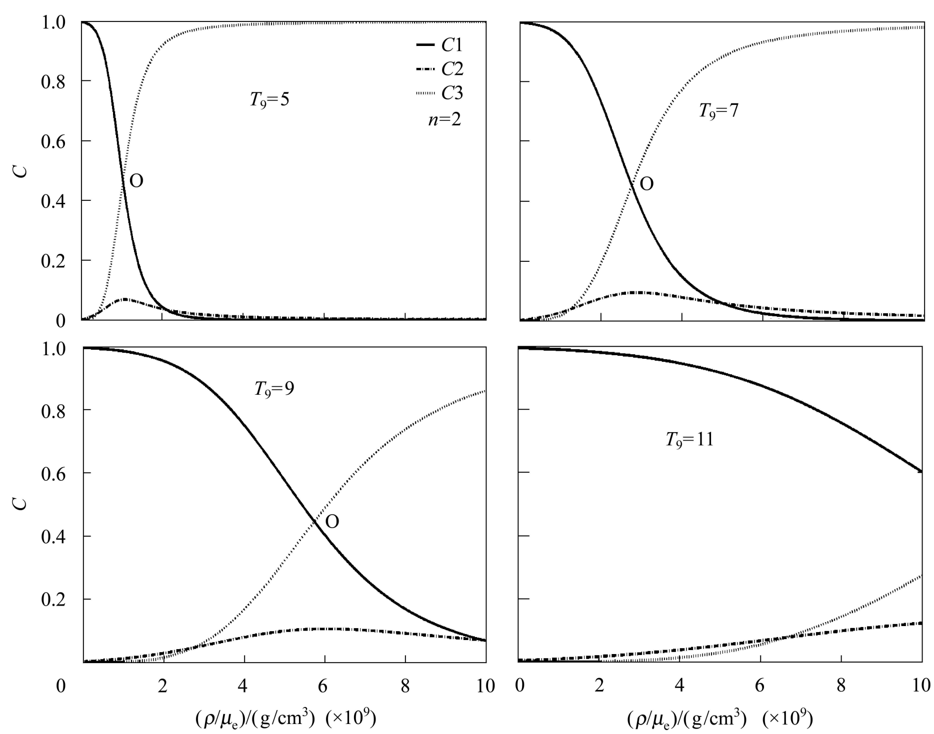

Fig. 2. Ratio factor C as a function of the density at the different temperatures T_9=5, 7, 9, 11.

4 Concluding remarks

Using the Weinberg-Salam theory, the competition of the NEL rates due to the pair, photo- and plasma neutrino process is canvassed. The pair NEL rate is constant at low density and decreases when the electrons become degenerate at high density. The photo-NEL rates are constant at very low density due to $e^{\pm}$ pair and decrease exponentially at very high densities. The plasma NEL rate is a strongly peaked function of ρ/μ_e and dominates the other two processes near its own peak. On the other hand the ratio factor C is very sensitive to the temperature and density. The ratio factor C_2 always is lower than the ratio factor C_1 and C_3. The pair NEL process is always the dominant contribution before the crossed point O. The plasma NEL process will be the main dominant contribution after the crossed point O. According to our calculations, the crossed point O which tells us the relation of $C_1 = C_3 = 0.45$, will move to the higher density direction with increasing of the temperature. The present results may have significant influence on further research of nuclear astrophysics and neutrino astrophysics, especially the research of the late stages of the stellar evolution.

References

1 Gamow G, Schonberg M. Phys. Rev., 1941, **59**: 539

2 Fuller G M, Fowler W A, Newman M J. AP. J, 1980, **42**: 447; Fuller G M, Fowler W A, Newman M J. AP. J, 1982, **252**: 715; Fuller G M, Fowler W A, Newman M J. AP. J, 1982, **48**: 279; Fuller G M, Fowler W A, Newman M J. AP. J, 1985, **293**: 1

3 LIU J J, LUO Z Q. Chinese Physics C (HEP & NP), 2008, **32**: 186

4 LIU J J, LUO Z Q, LIU H L, LAI X J. International Journal of Modern Physics A, 2007, **22**: 3305

5 LIU J J , LUO Z Q. Chinese Physics Letter, 2007, **24**: 1861

6 LIU J J , LUO Z Q. Chinese Physics, 2007, **16**: 3624

7 Esposito S, Mangano G, Miele G, Picardi I, Pisanati O. Nuclear Physics B, 2003, **658**: 217

8 Indranath Bhattacharyya J. Phys. G, 2006, **32**: 925

9 Beaudet G, Petrosian V, Salpeter E E. AP. J, 1967, **150**: 979

10 Dicus D A. Phys. Rev. D, 1972, **6**: 941

11 Munakata H, Kohyama Y, Naoki Itoh. AP. J, 1985, **296**: 197

12 Itoh N, Adachi T, Nakagawa M, Kohyama Y, Munakata H. AP. J, 1989, **339**: 354

13 Itoh N, Mutoh H, Hikita A, Kohyama Y. AP. J, 1992, **395**: 622

14 Itoh N, Hayashi H, Nishikawa A, Kohyama Y. AP. J, 1996, **102**: 411

15 Weinberg S. Phys. Rev. Letter, 1967, **19**: 1264

16 Salam A. Elementary Particle Physics. Ed. Svartholm N. 1968. 367

17 Kohyama Y, Itoh N, Munakata H. AP J, 1986, **310**: 810

18 Sirlin A. Phys. Rev. D, 1980, **22**: 971